

STAIN FUNGI CONTROL IN *PINUS* SP. WOOD WITH SILICA MESOPOROUS PARTICLES LOADED WITH ESSENTIAL OILS

TANIA MÉNDEZ-PÉREZ, MA. DEL CARMEN CHÁVEZ-PARGA, JARED MAYA-ALAVEZ, CRISANTO VELÁZQUEZ-BECERRA, JAIME ESPINO-VALENCIA, JOSÉ APOLINAR-CORTÉS, MAURO M. MARTÍNEZ-PACHECO
MICHOACAN UNIVERSITY OF SAINT NICHOLAS OF HIDALGO
MEXICO

(RECEIVED MAY 2023)

ABSTRACT

The use of essential oils (EO) carried onto mesoporous silica particles (MSPs) was tested to control pinewood stains. Three types of MSPs were synthesized and physicochemically characterized with N₂ physisorption (type IV), X-ray diffraction [Miller indices (100), (110), (200)], scanning electron microscopy, zeta potential (negative values), dynamic light scattering (< 200 nm) and thermogravimetric analysis (5% to 10% weight loss). A response surface design was used to find the EO loading conditions to control stain, the latter was measured as colour change with the CIEDE₂₀₀₀ formula. The essential oil loading onto MSPC was physicochemically confirmed by a weight loss of 47% in the thermogravimetric analysis. The Citrus, *Syzygium* sp. and *Tagetes* sp. oils carried onto mesoporous particles MSPC (30:1 w/w) controlled the pinewood stain caused by *Alternaria* sp. and *Geosmithia* sp. This was demonstrated by the absence of pigmentation and scarce fungal growth.

KEYWORDS: Wood stain, mesoporous silica particles, essential oils.

INTRODUCTION

Wood stain is caused by a heterogeneous fungal consortium, which varies depending on the wood extraction sites, the living history of the tree and species. Generally, wood stain does not affect the structure of the wood but causes aesthetic and economic losses (Komut 2022). The microbial decomposition of wood is controllable by an array of different organisms or their components. Sajitha et al. (2018) controlled sapstain on rubber wood caused by fungus

Lasiodiplodia theobromae with the use of *Bacillus subtilis*' secondary metabolites. Studies like this exhibit the potential use of secondary metabolites to control wood stains, also other fungi are sensitive to other plant bioactive compounds (Deresa and Diriba 2023).

Essential oils (EOs) are complex mixtures of plant secondary metabolites, abundant in e.g., terpenes, terpenoids and phenylpropenes. These components usually attach to the surface of microorganisms, penetrate the cell membrane, and cause their death (Jobdeedamrong et al. 2018). EOs are used in agricultural and biotechnological industries for their antifungal, antimicrobial and antioxidant activities. For instance, sapstain biocontrol in yellow pinewood (*Pinus* spp.) was achieved with *Pongamia pinnata* seed oil (Sahu et al. 2022). Likewise, components isolated from EOs such as cinnamaldehyde, eugenol and α -pinene inhibited yeast-like *Candida* spp. (Saracino et al. 2022). These show that EOs can control fungi that affect surfaces, namely, compact discs, parchment, and other forms of information storage (Cappitelli and Sorlini 2005), as well as, structural materials, such as wood. However, their physicochemical properties, including insolubility in water and instability, complicate their use (Jin et al. 2019). The loading of essential oils (EOs) within silica mesoporous particles (MSPs) protects their physicochemical and bioactive properties.

The advantages of MSPs are of interest to carry EOs because MSPs are mechanically resistant, chemically stable and biocompatible. Their applications are determined by properties, such as broad specific surface area, adjustable diameter and pore size. Complexes formed by mesoporous particles and EOs or their pure components are effective in growth control for problematic microorganisms (Bravo et al. 2018). Lu et al. (2020) reported an increase in the release time of citral from 5 h to 96 h when loaded onto mesoporous silica nanocolumns. This establishes the possibility of using MSPs as biocide agent carriers in agriculture, among other industries, like the wood industry. The interest in obtaining alternatives to synthetic chemical agents, that are environmentally friendly to control wood stains is still relevant. In this work, the use of EOs loaded onto MSPs is assessed to control wood stains by *Alternaria* sp. and *Geosmithia* sp. on *Pinus* sp. wood.

MATERIAL AND METHODS

Conservation and maintenance of the fungal isolates

Wood stain fungi *Alternaria* sp. and *Geosmithia* sp. were isolated from pinewood splinters from a pine beam with stain provided by the wooden collection of the Faculty of Engineering and Wood Technology in Michoacan University of Saint Nicholas of Hidalgo. Molecular methods identified the fungi until genre, and they were propagated in potato dextrose agar (Martínez-Pacheco et al. 2022).

Essential oils (EOs)

Syzygium sp. (clove) (SO) and citric (CO) essential oils were obtained from a local market. *Tagetes* sp essential oil (TO) was donated by Espinoza-Madriral (2019).

Analogue MCM-41 particle (MSP) synthesis

A hydrolysis/condensation particle synthesis was performed according to Ma et al. (2011). Briefly, 0.2 g of hexadecyltrimethylammonium bromide (CTAB) were diluted in 38.4 mL of deionized water by magnetic stirring at 400 rpm at 25°C. Afterwards, 13.6 mL of 96% ethanol and 4 mL of 29% ammonium hydroxide were added to the mixture and stirred at 400 rpm for 5 min. 3 mL of cyclohexane or 2.5 mL of benzene were added to the mixture as swelling agents and were mixed at 400 rpm for 5 min. Three types of particles were synthesized and designated as follows: MSP (without swelling agent), MSPC and MSPB (with cyclohexane and benzene as swelling agents, respectively). Subsequently, 1 mL of tetraethyl orthosilicate (TEOS) was added and stirring continued at 400 rpm for 3 h. The particles were recovered by vacuum filtration. Then were calcined at 540°C in a furnace for 9 h to remove the surfactant. The particles were kept in airtight glass containers.

MSP and pinewood probe characterization

Wood from *Pinus* sp. without any preservative treatment was collected from a local sawmill and fractioned in wooden blocks (probes) of uniform dimensions. MSPs diameters and superficial charges were determined through the dynamic light scattering (DLS) and zeta potential techniques (NanoBrook® 90 Plus). Suspensions of the samples were carried out in ultrafiltered deionized water at 2 ppm and were sonicated for 10 min (Branson® 2510). Pore diameter and size distribution were analyzed via nitrogen adsorption/desorption isotherms (Quantachrome® ASiQwin), with the mathematical model BJH and compared with the IUPAC classification of isotherms and hysteresis loops. The X-ray diffraction patterns (XRD) were obtained with a D8 Advance DAVINCI® diffractometer at low angles ($2\theta = 0^\circ$ to 5°) with $\text{CuK}\alpha$ as a radiation source ($\lambda = 1.5406 \text{ \AA}$). A thermogravimetric analysis (TGA) was performed on the particles with and without EO in a Simultaneous thermal analyzer (STA) 6000 with a heating ramp from 25°C to 550°C and 10°C/min heat steps. The results were expressed as relative weight. MSPs morphology and the surface of the probes after removing the fungi were analyzed via Scanning electron microscopy (SEM) (Jeol® JSM 7600F) at 5 kV. Before their analysis, the probes were covered with a copper layer by aspersion. The EOs composition was characterized by gas chromatography (CG Thermo Scientific model TRACE® 1310). Helium was used as the mobile phase. A 15 m long column, with a 0.25 mm internal diameter and a stationary phase layer of 0.25 μm was used. The chromatograms were analyzed with the software Xcalibur® (Thermo Scientific® 2019); they were compared with standards and the NIST® (2008) MS v.2.0. The reported compounds were the ones that met the following criteria: area percentage of ≥ 2 and a coincidence factor of ≥ 900 .

Loading of EOs onto MSPs

The EOs were loaded onto MSPs. Hexane was used as a solvent. 100 mg of MSP were stirred in a hexane and EO solution in an orbital shaker at 400 rpm at 25°C. An experimental design with the response surface method according to Khairudin et al. (2019) was used with three levels of EOs:MSPs ratios (10:1 w/w, 20:1 w/w or 30:1 w/w) and of time (12 h, 24 h or 36 h).

Evaluation of the control of pinewood stain from *Alternaria* sp. and *Geosmithia* sp. with EOs onto MSPs

Stain control was evaluated *in situ* on probes measuring 7 mm x 3 mm x 70 mm following the ASTM D4445-09 (2009) standard. They were sterilized at 121°C and 121 kPa for 20 min. After that, the probes were covered with a layer of MSPs loaded with EOs obtained in the previous experiment (4 mg MSPs). The MSPs from each treatment of the experimental design were applied on the probes, arranged in Petri dishes (90 mm x 15 mm), on glass slides (three probes per Petri dish). A 25 mm² inoculum from the fungi was added to each probe and they were incubated at 25°C for 4 weeks. The probes with MSPC+CO were inoculated with *Geosmithia* sp. and the ones with MSPC+SO and MSPC+TO were inoculated with *Alternaria* sp. Probes treated with hexane, 4 mg of empty MSPs, 1.8 mg non-loaded EO and 2% (w/v) OPP were used as controls. Humidity in the Petri dishes was maintained with filter paper dampened with sterile deionized water. The colour of the probes was measured with a colour meter (TES® 135A) in the following stages: after sterilization, after the addition of the MSPs and after removing the inoculum from the probes. Three colour measurements were made on each probe using the CIE L*a*b* coordinates. The colour difference (ΔE) was calculated with the software R using the CIEDE₂₀₀₀ formula (Luo et al. 2001). The code programmed for this experiment was published on RPubS by Méndez-Pérez (2021).

Statistical analysis

All experiments were performed in duplicate. The results are shown as mean \pm standard error. The software Statistica© v.8 was used to obtain the significance of the data.

RESULTS AND DISCUSSION

Physicochemical characterization of MSPs and EOs

Growth of chromogenic fungi is a relevant problem that has not been solved. Essential oils inhibit the growth of stain fungi such as *Alternaria* sp. and *Geosmithia* sp. Loading EOs onto mesoporous particles is an alternative to extend their biocide action.

Three types of particles were obtained with different swelling agents and were physicochemically characterized. They showed Type IV isotherms (Fig. 1a) with type A (or H1) hysteresis and tubular pores. MSPs exhibited a specific surface area of 1 235.20 m²/g and a pore volume of 0.83 cm³/g. This result is similar to the physicochemical parameters reported for MCM-41 particles (Shao et al. 2020). Swelling agents cyclohexane or benzene produced particles with disordered pore structures (Popa et al. 2020) as shown in Fig. 1d. Mean pore diameter of 2.20 nm was similar in MSPB and MSP. Pore size distribution was uniform for MSPs, but it was not uniform for MSPC and MSPB. This pore size distribution was attributed to the swelling agent being introduced into some micelles and not in others. Similarly, trimethyl benzene (TMB) as a swelling agent produced different pore diameters in mesoporous hydroxyapatite particles (Zeng et al. 2014). The X-ray diffraction analysis (Fig. 1b) for the MSP showed the typical pattern for a hexagonal array of MCM-41 particles.

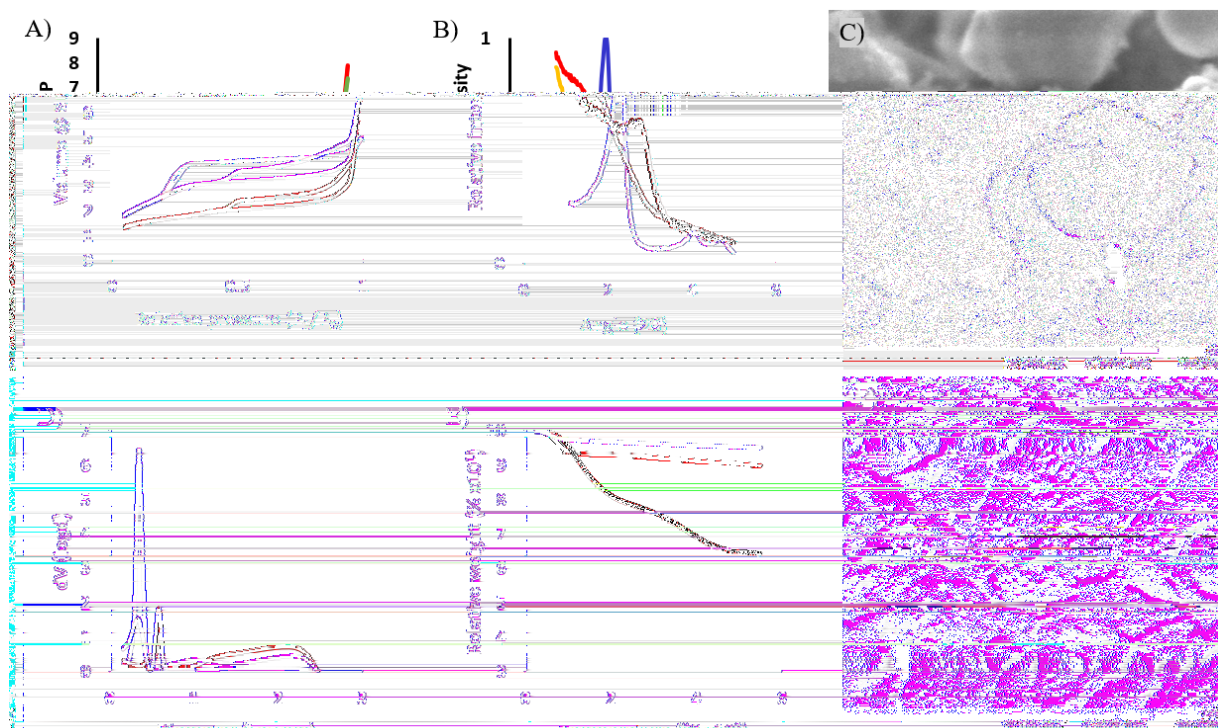


Fig. 1: Characterization of the MSPs and MSPC+CO particles: a) N_2 adsorption isotherms, b) X-ray diffraction, c) SEM of MSPC without EO, d) pore size distribution, e) thermogravimetric analysis, and f) SEM of MSPC with EO. The colour blue, red, green and yellow represents MSP, MSPC, MSPB, and MSPC+CO, resp.

The values of zeta potential (Fig. 3) for the MSP, MSPC and MSPB were in the stability interval (instability interval is -30 mV to 30 mV). The negative values of zeta potential on the surface of MSPs are a consequence of silanol groups, which were also observed on mesoporous silica particles with three different pore sizes (2 nm, 5 nm and 10 nm) (Ahn and Kwak 2020). The morphologies of MSPC without EO (Fig. 1c) were observed by scanning electron microscopy. The particles exhibited a semispherical shape: the MSPC diameters were between 200 nm and 400 nm.

Thermogravimetric analysis was done for the MSP and MSPC (Fig. 1e). The MSPs lost approximately 5% of their total weight. The weight loss at 100°C is a consequence of the loss of water physisorbed on the surface. A similar result for MCM-41 particles was reported by Hachemaoui et al. (2020).

The antifungal effect of the EOs depends on their composition and quantity of active molecules. The gas chromatograms of the EOs (Fig. 2) show the major components of the CO (Fig. 2a). *D*-limonene stood out with a relative abundance of 47.34%. While α and β -pinene, γ -terpinene and terpinolene were 7.39%, 21.35%, 15.34% and 3.01%, resp. *D*-limonene is a monoterpene that inhibits the growth of a wide variety of fungi by damaging the cell membrane (Sattary et al. 2020). In the SO chromatogram (Fig. 2b) the major components were eugenol (52.89% relative abundance), caryophyllene (14.17%), eugenol acetate (12.89%), humulene (5.89%) and caryophyllene oxide (3.02%). Eugenol is effective as an antifungal because it inhibits ergosterol synthesis, altering the cytoplasmic membrane (Li et al. 2021).

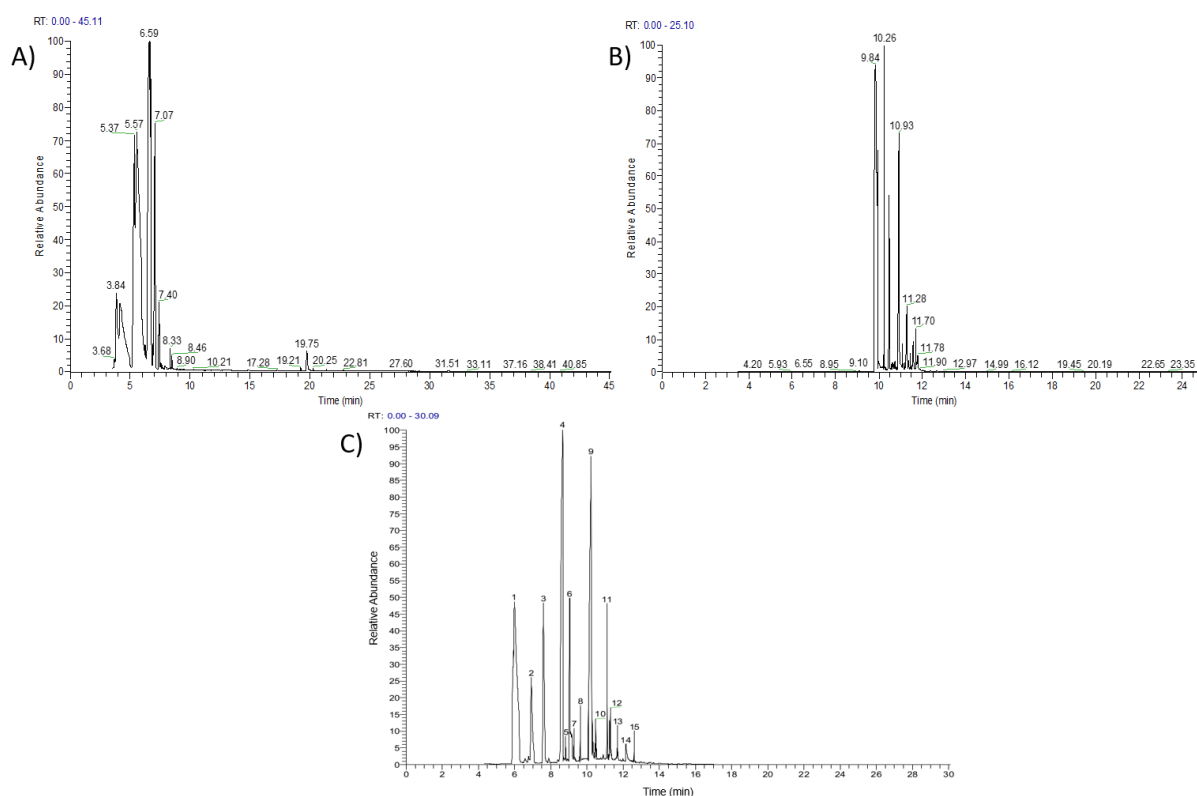


Fig. 2: Chromatographic profile of the EOs via gas chromatography: a) CO, b) SO, and c) TO.

The TO (Fig. 2c) presented estragole and methyleugenol as major components with 26.96% and 24.55% relative abundance, respectively. Also, β -pinene, linalool, β -ocimene, geraniol and *trans*-nerolidol, with relative abundances of 15.07%, 10.05%, 6.46%, 6.25% and 3.28%, respectively. The fungi *Microsporium canis* and *Alternaria* sp. were inhibited with EO from *Tagetes* sp. composed of 83% of estragole (Bandeira Reidel et al. 2018).

Influence of the swelling agents on the particle size and zeta potential in loading of EOs onto MSPs

To know the interaction between variables while looking for a more significant antimicrobial effect in the loading of EO onto MSPs, response surface experimental designs were used. Yue et al. (2020) used this methodology to inhibit *Botrytis cinerea* with tea tree EO and cyclodextrins. The experimental design was used to select the loading conditions of the essential oil that resulted in the most significant stain control on pinewood.

The influence of the swelling agents on the way the EOs are carried onto the MSPs was analyzed. Changes in particle size and zeta potential indicate the adhesion of the EOs on the surface of the particles or inside the material's pores (Fig. 3). Based on this we selected the MSPC to fulfil the purpose of this work. Since the zeta potential values of the MSPC+CO were similar to the values of the empty MSPC. The inference is that particle's surface did not present a layer of oil, and the particles carried the oil inside their pores. On the other hand, the zeta potential values of the MSP changed, which infers the formation of an oil layer

on the particles. This fact does not allow for the control of the quantity of EO carried on the particle (Gao et al. 2019).

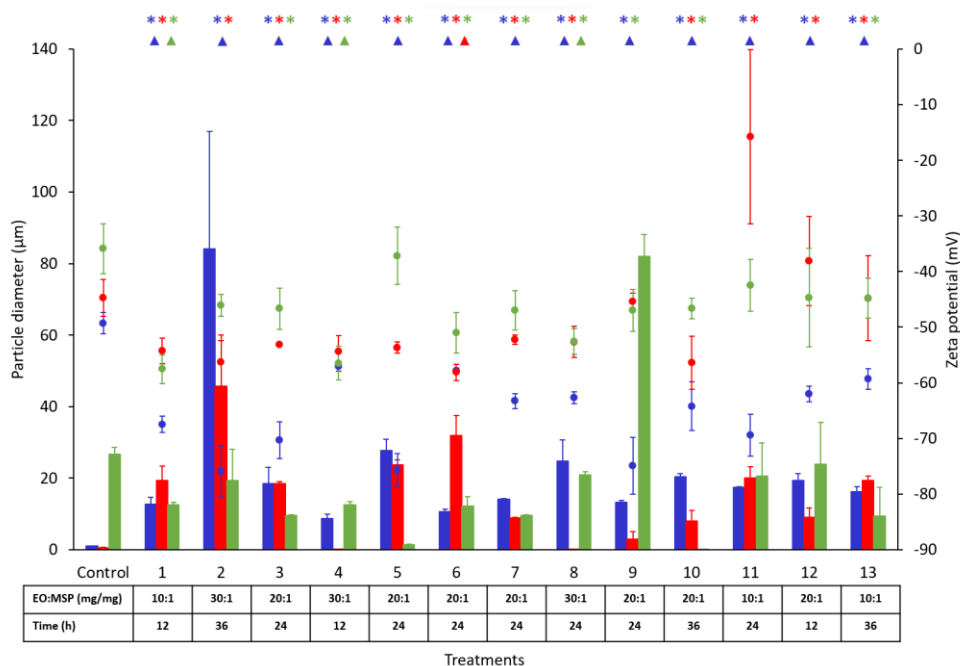


Fig. 3: Influence of the swelling agents on the particle size and zeta potential in loading the EOs onto MSPs. The particle diameter (bars) and zeta potential (dots) values of MSP, MSPC and MSPB are represented in colour blue, red, and green, respectively. The results are the mean of a $n = 3 \pm SE$. *Indicates significant difference in particle diameter between the control and the treatment. t -Student $p > 0.05$. ▲Indicates significant difference in zeta potential between the control and the treatment. t -Student $p > 0.05$.

The MSPC were characterized after the addition of the CO to further confirm its presence inside the pores. In the X-ray diffractogram for MSPC (Fig. 1b) the Bragg reflections were modified, meaning that the structure is irregular. MSPC+CO showed a diffraction pattern similar to MSPC. Poyatos-Racionero et al. (2021) obtained comparable diffractograms with MCM-41 particles loaded with carvacrol, cinnamaldehyde, and thymol. The change in the Bragg reflections is due to the quantity of organic matter (EO) inside the material's pores. The surface of the MSPC+CO (Fig. 1f) presented roughness attributed to oil adhesion on the particles. According to TGA analysis, 47% of the total weight of the MSPC+CO particles is EO. This proves the presence of the oil in the particles.

Loading conditions of the EOs onto MSPC and control of stain in *Pinus* sp.

The loading conditions of the EOs onto the MSPC were selected based on the results shown in Fig. 4. The factors considered were the EO:MSPC ratio and the time of interaction between EOs and MSPs. The colour change (ΔE) was the criterion for measuring the stain control on the probe. The anti-stain effect on pinewood was performed with MSPCs loaded with CO, TO and SO. The results using MSPC+CO (Fig. 3c) exhibited a lower change of colour when the EO:MSPC ratio was 30:1 w/w. The MSPC+TO showed similar behaviour with a stronger

influence of time: 12 h were adequate for interaction. The photographs of the probes after treatment with MSPC+EO showed control of stain with the three oils. The loaded EOs had better control of the stain than the non-loaded oils on pinewood. The three EOs loaded onto MSPC had similar effects in the control of wood stain (Fig. 4). The treatments that resulted in less stain on pinewood were: 11 for MSPC+SO, 8 for MSPC+TO and 4 for MSPC+CO. Delta E values reached lower levels with MSPC+TO.

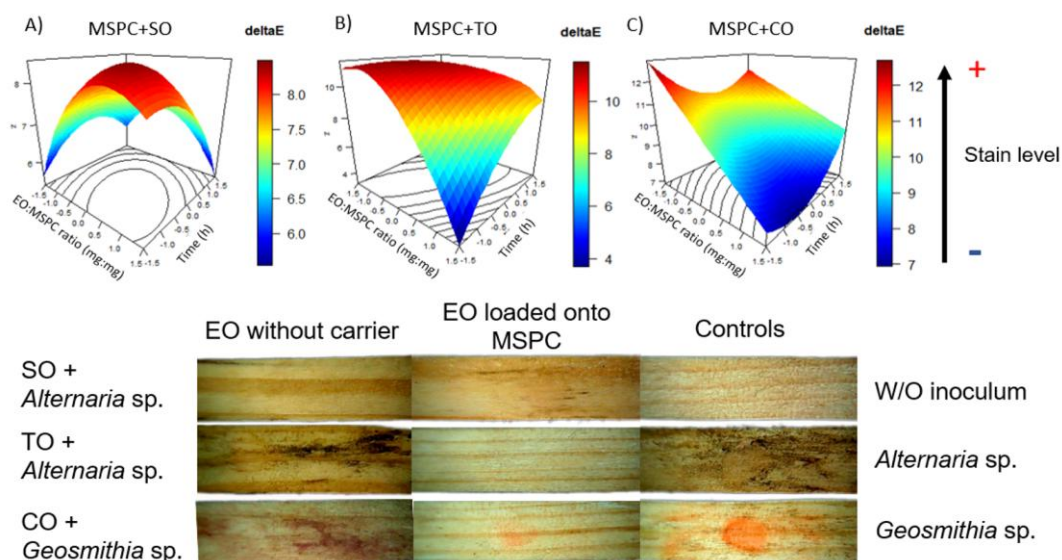


Fig. 4: Selection of the loading conditions of the EOs onto the MSPC for stain control on *Pinus* sp. probes. Panels A, B and C show the response surface graphs that resulted from the experimental design for SO, TO and CO, respectively. The colour blue represents low stain and the colour red represents high stain. The photographs show representative probes of the treatments with EOs without a carrier, the treatments with loaded EOs and the controls (without inoculum, inoculated with *Alternaria* sp. and with *Geosmithia* sp.).

Control of the development of *Geosmithia* sp. on the surface of *Pinus* sp. treated with MSPC+CO

The SEM images (Fig. 5) after the treatment of the probes with MSPC+CO showed the absence of fungal growth and pigmentation. A decrease in fungal biomass was observed (Figs. 5c,d,f). A scarce quantity of conidia (marked with red arrows) was found in the treated probes. The effectiveness of the MSPC in carrying EO was demonstrated. Therefore, stain control on probes was achieved because the fungi *Alternaria* sp. and *Geosmithia* sp. are sensitive to the three EOs studied.

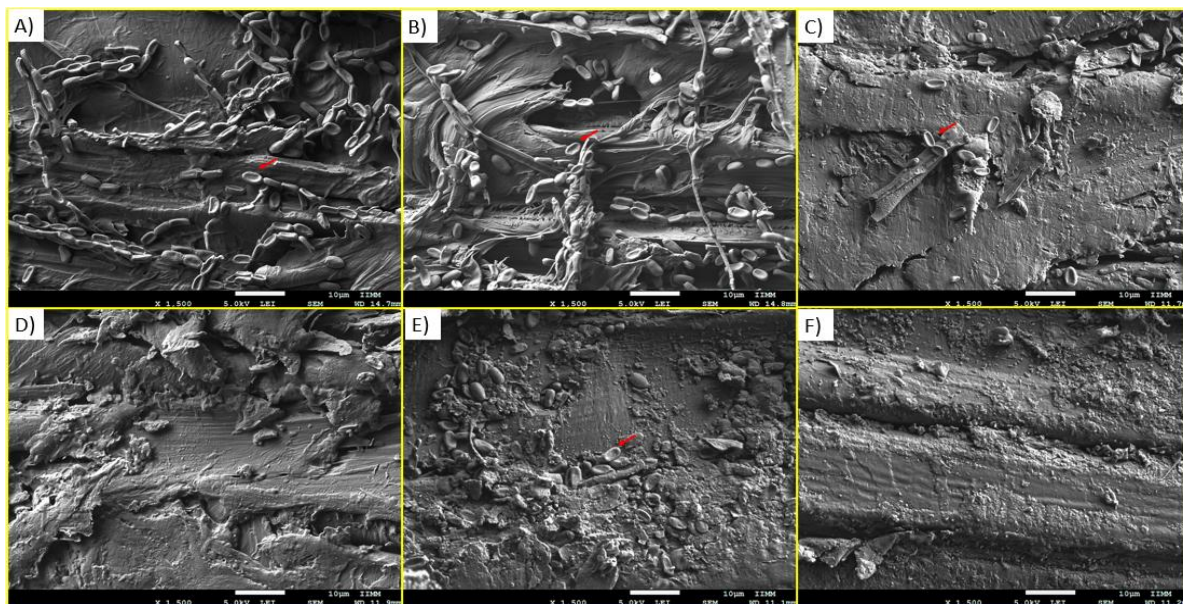


Fig. 5: *Geosmithia* sp. development on the surface of *Pinus* sp. treated with MSPC+CO (SEM at 1 500 x). Probes inoculated with the fungus: a) without treatment, b) with hexane, c) with non-loaded oil, d) with MSPC+CO treatment 4, e) with MSPC+CO treatment 1 and f) non-inoculated.

Panel D stood out, it corresponds to treatment 4, in which the MSPC:EO ratio was 30:1 w/w and the interaction time for the loading of EO was 12 h. This evidence exhibited that the CO loaded onto MSPCs prevented the adherence of the fungus to the surface of the wood and consequently, controlled the stain on the probes.

CONCLUSIONS

The essential oil loading onto MSPC was physicochemically confirmed by a weight loss of 47% in the thermogravimetric analysis. The Citrus, *Syzygium* sp. and *Tagetes* sp. oils carried onto mesoporous particles MSPC (30:1 w/w) controlled the pinewood stain caused by *Alternaria* sp. and *Geosmithia* sp. This was demonstrated by the absence of pigmentation and scarce fungal growth.

ACKNOWLEDGMENTS

Thanks to UMSNH for partial funding. TMP and JMA obtained a CONAHCyT scholarship.

REFERENCES

1. AHN, Y. & KWAK, S.Y. (2020): Functional mesoporous silica with controlled pore size for selective adsorption of free fatty acid and chlorophyll. In: *Microporous and Mesoporous Materials* 306, 110410.
2. ASTM D4445-09, 2009: Standard test method for fungicides for controlling sapstain and mould on unseasoned lumber (laboratory method).
3. BANDEIRA REIDEL, R.V., NARDONI, S., MANCIANTI, F., ANEDDA, C., GENDY, A.E.G. EL, OMER, E.A. & PISTELLI, L. (2018): Chemical composition and antifungal activity of essential oils from four Asteraceae plants grown in Egypt. In: *Zeitschrift für Naturforschung* 73 (7-8), 313–318 pp.
4. BRAVO C.M., PRESTON, G.M., VAN DER HOORN, R.A.L., TOWNLEY, H.E. & THOMPSON, I.P. (2018): Species-specific antimicrobial activity of essential oils and enhancement by encapsulation in mesoporous silica nanoparticles. In: *Industrial Crops and Products* 122, 582–590 pp.
5. CAPPITELLI, F. & SORLINI, C. (2005): From papyrus to compact disc: The microbial deterioration of documentary heritage. In: *Critical Reviews in Microbiology* 31(1), 1 -10 pp.
6. DERESA, E.M., DIRIBA, T.F. (2023): Phytochemicals as alternative fungicides for controlling plant diseases: A comprehensive review of their efficacy, commercial representatives, advantages, challenges for adoption, and possible solutions. In: *Heliyon* 9(3), e13810.
7. ESPINOZA-MADRIGAL, R.M. (2019): Control de la pudrición peduncular del fruto de aguacate (*Persea americana* Mill. cv Hass) con derivados vegetales. Ph. D. Thesis. Universidad Michoacana de San Nicolás de Hidalgo. Morelia, Michoacán. México. 31-32 pp.
8. GAO, F., ZHOU, H., SHEN, Z., QIU, H., HAO, L., CHEN, H. & ZHOU, X. (2019): Synergistic antimicrobial activities of tea tree oil loaded on mesoporous silica encapsulated by polyethyleneimine. In: *Journal of Dispersion Science and Technology* 41(12), 1859-1871 pp.
9. HACHEMAOUI, M., BOUKOUSSA, B., MOKHTAR, A., MEKKI, A., BELDJILALI, M., BENAÏSSA, M., ZAOUÏ, F., HAKIKI, A., CHAÏBI, W., SASSI, M. & HAMACHA, R. (2020): Dyes adsorption, antifungal and antibacterial properties of metal loaded mesoporous silica: Effect of metal and calcination treatment. In: *Materials Chemistry and Physics* 256, 123704.
10. JIN, L., TENG, J., HU, L., LAN, X., XU, Y. (2019): Pepper fragrant essential oil (PFEO) and functionalized MCM-41 nanoparticles: formation, characterization, and bactericidal activity. In: *Journal of the Science of Food and Agriculture* 99(11), 5168-5175 pp.
11. JOBDEEDAMRONG, A., JENJOB, R., CRESPIY, D. (2018): Encapsulation and release of essential oils in functional silica nanocontainers. In: *Langmuir* 34(44), 13235-13243 pp.
12. KHAIRUDIN, N.H., NOR, Y.A. & HASHIM, Y.Z.H. (2019): Rough hollow mesoporous silica nanoparticles as carrier for agarwood oil to treat cancer cells. In: *Journal of Advanced Research in Materials Science* 54(1), 1–9 pp.
13. KOMUT, O. (2022): Blue stain in lumber industry and losses caused by cutting methods. In: *Wood Research* 65(6), 303-312 pp.

14. LI, Y., ZHAO, R., LI, Y. & ZHOU, Z. (2021): Limonin enhances the antifungal activity of eugenol nanoemulsion against *Penicillium italicum* in vitro and in vivo tests. In: *Microorganisms* 9(5), 969.
15. LU, Z., WANG, X., ZHANG, T., XIAO, Z., YANG, J., NIU, Y., WANG, J., LIU, G., SHEN, J. & ZHANG, X. (2020): Effect of mesoporous silica nanoparticles-based nano-fragrance on the central nervous system. In: *Engineering in Life Sciences* 20(11), 535-540 pp.
16. LUO, M.R., CUI, G. & RIGG, B. (2001): The development of the CIE 2000 colour-difference formula: CIEDE2000. In: *Color Research and Application* 26 (5), 340-350 pp.
17. MA, S., WANG, Y. & ZHU, Y. (2011): A simple room temperature synthesis of mesoporous silica nanoparticles for drug storage and pressure pulsed delivery. In: *Journal of Porous Materials* 18, 233–239 pp.
18. MARTÍNEZ-PACHECO M.M., GARCÍA REYNOSO W.E., CRUZ DE LEÓN J., RAYA GONZÁLEZ D., FLORES GARCÍA A., MUNRO ROJAS A. & VELÁZQUEZ BECERRA C. (2022): Pinewood protection against sapstain using citrus essential oils. In: *Revista Árvore* 46, 4616.
19. MÉNDEZ-PÉREZ, T. (2021). CIEDE 2000 color difference calculator.
20. POPA, A., BORCANESCU, S., HOLCLAJTNER, I., DANICA, A. & BOGDANOVIĆ, B. (2020): Preparation and characterisation of aminofunctionalized pore expanded mesoporous silica for carbon dioxide capture. In: *Journal of Porous Materials* 28, 143-156 pp.
21. POYATOS-RACIONERO, E., GUARÍ-BORRÀS, G., RUIZ-RICO, M., MORELLÁ-AUCEJO, Á., AZNAR, E., BARAT, J.M., MARTÍNEZ-MÁÑEZ, R., MARCOS, M.D. & BERNARDOS, A. (2021): Towards the enhancement of essential oil components' antimicrobial activity using new zein protein-gated mesoporous silica microdevices. In: *International Journal of Molecular Sciences* 22(7), 3795.
22. SAHU, A., TRIPATHI, S., GANGULY, S. & SUMI, A. (2022): Fumigation of imported *Tectona grandis* and southern yellow pine with *Pongamia pinnata* seed oil against sapstain and mould. In: *Maderas: Ciencia y Tecnología* 24(6), 1-12 pp.
23. SAJITHA, K.L., DEV, S.A. & FLORENCE, E.J.M. (2018): Biocontrol potential of *Bacillus subtilis* B1 against sapstain fungus in rubber wood. In: *European Journal of Plant Pathology* 150, 237–244 pp.
24. SARACINO, I.M., FOSCHI, C., PAVONI, M., SPIGARELLI, R., VALERII, M.C. & SPISNI, E. (2022): Antifungal activity of natural compounds vs. *Candida* spp.: A mixture of cinnamaldehyde and eugenol shows promising in vitro results. In: *Antibiotics* 11(1), 73.
25. SATTARY, M., AMINI, J. & HALLAJ, R. (2020): Antifungal activity of the lemongrass and clove oil encapsulated in mesoporous silica nanoparticles against wheat's take-all disease. In: *Pesticide Biochemistry and Physiology* 170, 104696.
26. SHAO, P., CHEN, H., YING, Q. & ZHANG, S. (2020): Structure-activity relationship of carbonic anhydrase enzyme immobilized on various silica-based mesoporous molecular sieves for CO₂ absorption into a potassium carbonate solution. In: *Energy Fuels* 34(2), 2089–2096 pp.

27. YUE, Q., SHAO, X., WEI, Y., JIANG, S., XU, F., WANG, H. & GAO, H. (2020): Optimized preparation of tea tree oil complexation and their antifungal activity against *Botrytis cinerea*. In: Postharvest Biology and Technology 162, 111114.
28. ZENG, F., WANG, J., WU, Y., YU, Y., TANG, W., YIN, M. & LIU, C. (2014): Preparation of pore expanded mesoporous hydroxyapatite via auxiliary solubilizing template method. In: Colloids Surfaces A: Physicochemical and Engineering Aspects 441, 737–743 pp.

TANIA MÉNDEZ-PÉREZ, MA. DEL CARMEN CHÁVEZ-PARGA*,
JAIME ESPINO VALENCIA, JOSÉ APOLINAR-CORTÉS
MICHOACAN UNIVERSITY OF SAINT NICHOLAS OF HIDALGO
CHEMICAL ENGINEERING FACULTY'S POSTGRADUATE STUDIES DIVISION
S/N FRANCISCO J. MÚGICA AVENUE, UNIVERSITY CAMPUS
58030 MORELIA, MICHOACAN
MEXICO

*Corresponding author: cparga@umich.mx

JARED MAYA-ALAVEZ, CRISANTO VELÁZQUEZ-BECERRA
MICHOACAN UNIVERSITY OF SAINT NICHOLAS OF HIDALGO
FACULTY OF ENGINEERING AND WOOD TECHNOLOGY
S/N FRANCISCO J. MÚGICA AVENUE, UNIVERSITY CAMPUS
58030 MORELIA, MICHOACAN
MEXICO

MAURO M. MARTÍNEZ-PACHECO*
MICHOACAN UNIVERSITY OF SAINT NICHOLAS OF HIDALGO
CHEMICO-BIOLOGICAL INVESTIGATIONS INSTITUTE
S/N FRANCISCO J. MÚGICA AVENUE, UNIVERSITY CAMPUS
58030 MORELIA, MICHOACAN
MEXICO

*Corresponding author: mpacheco@umich.mx